Role of Antibody Paratope Conformational Flexibility in the Manifestation of Molecular Mimicry

Lavanya Krishnan, Gaurav Sahni, Kanwal J. Kaur, and Dinakar M. Salunke
National Institute of Immunology, New Delhi, India

ABSTRACT Molecular mimicry is a recurrent theme in host defense processes. The correlation of functional mimicry with the structural features of the antibody paratope has been investigated, addressing the consequences of mimicry in host immune mechanisms. Two anti-mannopyranoside antibodies, 1H7 and 2D10, representing the possible extremes of the recognition spectrum with regard to peptide-carbohydrate mimicry were examined. Crystallographic and molecular dynamics simulation analyses established correlation between the antibody flexibility and the manifestation of mimicry. It was evident that monoclonal antibody (mAb) 1H7, which has a narrow specificity in favor of the immunizing antigen, exhibited structural invariance. On the other hand, the antigen-combining site of 2D10, the mimicry-recognizing antibody, showed substantial divergence in the complementarity determining region loops. The docking of mannopyranoside within the antibody paratope revealed multiple modes of binding of the carbohydrate antigen in mAb 2D10 vis à vis single docking mode in mAb 1H7, which overlapped with the common monosaccharide binding site defined in anti-carbohydrate antibodies. The presence of additional antigen binding modes is perhaps reflective of the utilization of conformational flexibility in molecular mimicry. A relatively broader recognition repertoire—attributable to paratope flexibility—may facilitate the recognition of altered antigens of invading pathogens while the antibodies with narrow recognition specificity maintain the fidelity of the response.

INTRODUCTION

The hallmark of the acquired immune system is remarkable specificity in its recognition repertoire that not only counters the invading pathogens but also ensures self-nonself discrimination. Studies involving various aspects of humoral and cellular immunity have enormously contributed to our present view of the specificity and complexity of molecular recognition. Although resemblance between antigenic determinants of the invading pathogen and the host may be critical for entry and manipulation of host cellular mechanisms, immune mechanisms have evolved toward fine discrimination between molecules which may otherwise appear similar. Molecular mimicry, in essence, is the antithesis of the specificity of antigen recognition and is the central premise implicated in the etiology and pathogenesis of autoimmunity (1,2).

Since molecular recognition is mediated by a combination of weak noncovalent interactions, structural similarity between antigens has often been thought to be the basis of molecular mimicry. However, functional correlation without adequate topological similarity has indeed been demonstrated (3–5). The emerging dichotomy enforces exploration of other physicochemical properties of the mimotopes as well as receptors in describing the basis of mimicry. Delineation of the molecular mechanisms associated with the recognition of chemically independent yet mimicking antigens is therefore crucial for a better understanding of mimicry in the immune response.

Mimicry between the carbohydrate moiety, methyl-α-D-mannopyranoside, and the Tyr-Pro-Tyr motif containing peptides has been extensively addressed in this laboratory using concanavalin A as a common receptor (6–9). The carbohydrate antigen and its mimicking 12-mer peptide (DVFYPYPYASGS) were established to be equivalent in terms of the physiological responses generated against either of them (10,11). Functional equivalence between the antigens was observed not only in terms of cross-reactivity but also during maturation of the antibody response and generation of immune memory. Toward molecular depiction of the functional mimicry, a panel of monoclonal antibodies (mAbs) was generated against mannopyranoside (12). Kinetic and thermodynamic investigations of antigen binding to these mAbs indicated the possible role of conformational flexibility in the manifestation of mimicry.

The studies presented here address the immune mechanisms implicated in molecular mimicry. We attempted to discern the structural properties associated with the manifestation of mimicry using a set of independent antibodies which differed in their ability to recognize a pair of mimicking antigens, a carbohydrate and a peptide. Crystallographic and in silico analyses of the anti-mannopyranoside antibodies, 1H7 and 2D10, demonstrate the overwhelming influence of the structural properties of the paratope in modulating molecular mimicry in the antibody response. It was revealed that the manifestation of functional mimicry is associated with flexibility in the antibody paratope and can be correlated with the differential modes of antigen binding.

Submitted March 9, 2007, and accepted for publication September 12, 2007.

Address reprint requests to Dinakar M. Salunke, National Institute of Immunology, Aruna Asaf Ali Road, New Delhi 100 067, India. Tel.: 91-11-2671-7113 91-11-2670 3686; Fax: 91-11-2671-7113; E-mail: dinakar@nii.res.in.

Editor: Ivet Bahar.

0006-3495/08/02/1367/10 $2.00

doi: 10.1529/biophysj.107.108654

MATERIALS AND METHODS

Generation of mAbs and Fab fragments

The anti-mannopyranoside mAbs used in this study were generated previously from an immune response against mannopyranoside-keyhole limpet hemocyanin (12). Purification of the antibodies, 1H7 and 2D10, from ascites was carried out following a two-step protocol that involved an initial partial purification with 40% ammonium sulfate fractionation followed by ion exchange chromatography on a diethylaminoethyl (DEAE) anion exchange column on high performance liquid chromatography.

Fab fragment was generated by papain digestion of the purified antibody in 100 mM TrisCl, pH 7.1 with 150 mM NaCl, and purified from the digestion mix by using DEAE anion exchange chromatography. The purity was checked by sodium dodecylsulfate-polyacrylamide gel electrophoresis, and the concentration of the Fab was estimated by protein assay (Bio-Rad, Hercules, CA) by using bovine serum albumin as the standard. The concentrated (10 mg/ml) Fab was dialyzed against the crystallization buffer, 50 mM TrisCl, pH 7.4, and/or 50 mM cacodylate, pH 6.8 with 0.05% sodium azide.

Crystallization and data collection

For crystallization of mAb 1H7, hanging drops containing 3–5 μl of 1H7 Fab and equivalent volume of the precipitant were set up at 25°C with and without 25 molar excess of mannopyranoside. The crystals were cryoprotected by soaking in mother liquor containing 25% glycerol and flash frozen. Data were collected on a MAR345dtb image plate (Marresearch, Norderstedt, Germany) installed on a rotating anode x-ray source (Rigaku, Tokyo, Japan) operating at 5.0 kW at 120 K and processed and scaled with AUTOMAR (Marresearch).

Structure determination and refinement

The structure was determined by molecular replacement using AmoRe (13). Anti-arsonate antibody 36–71 (Protein Data Bank (PDB) ID: 6FAB) was used as the probe model as the intensity data gave a correlation coefficient of 32.8% and R-factor of 46.3%. The light and heavy chains were defined as L and H, respectively, in one molecule in the asymmetric unit and as A and B, respectively, in the other. Subsequent refinement with CNS (14) was conducted by using this model and conventional R_{cryst} and R_{free} (10% of total reflections) values were monitored (15). Rigid body refinement was first carried out for the individual Fab molecules, and then the VH, VL, CH, and CL domains were treated as discrete units followed by iterative positional refinement. Electron density maps were displayed with the help of program O (16), and the sequence of antibody 36–71 was slowly changed to that of mAb 1H7 and water molecules added. The overall quality of the model was evaluated with PROCHECK (17); 96.7% residues are in the allowed regions of the Ramachandran plot, 2.5% in the generously allowed and 0.8%, including L56N (complementarity determining region (CDR) L2), H102W (CDR H3), A53A (CDRL2), and B105A (CDR H3), in the disallowed regions.

The structural data, including amplitudes and phases, and the derived coordinates of the Fab fragment of the mAb 1H7 are deposited at the PDB (Accession No. 2V7H).

Molecular modeling

For homology modeling of anti-mannopyranoside antibody 2D10, the structure of anti-digoxin Fab (PDB ID: 1IGI) was used as template; it showed maximum sequence identity with both heavy and light chains. Since we were primarily studying the antigen binding site and its interactions with the ligand, only the variable regions of the antibody were modeled using the HOMOLOGY module of INSIGHT II (Accelrys, 1998). Subsequently, the structure of 2D10 Fv was energy minimized in the DISCOVER module of INSIGHT II with 100 steps of steepest descent minimization followed by 400 steps of conjugate gradient minimization with gradually decreasing tethering to the backbone of the structure in AMBER force field. The final model was validated by PROCHECK (17). Of the 230 residues of 2D10, Fv 98% are in the allowed regions of the Ramachandran plot, 1.0% in the generously allowed and 1.0%, Val-56 (CDR L2) and Tyr-213 (CDR H3), in the disallowed regions.

Molecular dynamics simulation

All MD simulations of the variable regions of the anti-mannopyranoside mAbs were carried out using explicit solvent with an 8 Å water box beyond the Fv boundary at 16°C and 35°C in the SANDER program of the AMBER7 package for the duration of 500 ps and AMBER9 for the 2 ns simulations (18). To correlate with the previous thermodynamic analyses (12), the reference temperature for MD simulation was set at 16°C. The simulations were carried out keeping the volume constant with a time step of 2 fs (using SHAKE) and a cutoff of 8 Å. This was exclusive of an initial 25 ps equilibration, wherein all atoms were constrained by a harmonic potential, with a force constant of 5 kcal/mol/Å.^{2} Thereafter only the Cα atoms of the framework regions of the two antibodies were tethered keeping all atoms of the CDR loops free, thus permitting an exhaustive exploration of possible paratope conformations. Energy variation during the first 100 ps was monitored to ensure that the structures were optimized. Structure outputs were taken from the simulation every 0.2 ps, and energy minimization (100 steps of steepest descent minimization followed by 400 steps of conjugate gradient minimization in AMBER) and analyses were done for structures output every 10 ps. The ensemble of structures was visualized and root mean-square deviation (RMSD) of the Cα atoms of the CDR loops was calculated.

Automated docking of mannopyranoside and glucopyranoside

The program AUTODOCK3.05 is an automated procedure for predicting where a ligand binds on the surface of a macromolecule on the basis of the interaction between the two (19). AUTODOCK3.05 treats the macromolecule as rigid, whereas the ligand is allowed torsional flexibility. The Lamarckian genetic algorithm (LGA) is most efficient in searching the conformational space for the best docking energy (19). As an input, the Fv fragment of the antibodies were provided to the program with a rectangular box, a grid of 70 points in three dimensions with a spacing of 0.375 Å centered at the coordinates of the antigen-combining site, within which the program finds the binding site. Rigidity of the paratope during docking does not detract from its validity as multiple conformations of the antibody generated during MD simulation, for both ''rigid'' 1H7 Fv (with altered side-chain conformation of HTyr-106) and the ''flexible'' mAb 2D10, have been used to carry out multiple runs of the program.

For either antibody, docking of mannopyranoside and glucopyranoside was attempted on 11 different structures output every 50 ps during the course of the MD simulation. The default settings of AUTODOCK3.05 were used, with the exception of the number of runs, which was set to 100. AUTODOCK3.05 provides a comprehensive view of the available ligand docking sites and additionally calculates the docking and interaction energies as well as the theoretical affinity of the interaction of the ligand at each docking position. No external bias can be applied to steer the selection of the docking sites, except by exclusion from the grid frame, within the protein. In this study, all docking options (~15%) that were found to be outside of the antibody paratope were regarded as nonphysiological and therefore omitted from our analysis. Analysis of the docking energy of individual docking options was carried out to evaluate the affinity of mannopyranoside or glucopyranoside.

RESULTS

Antigen-free states of the anti-mannopyranoside mAbs

From the panel of anti-mannopyranoside mAbs, two antibodies, 1H7 and 2D10, which appeared to represent apparent

extremes of specificity of antigen recognition, were analyzed at the structural level. Although mAb 1H7 was highly specific to the mannopyranoside immunogen, mAb 2D10 recognized both the carbohydrate and its mimicking peptide with similar affinities (12). Fab was generated for the antibodies, and crystallization attempts included both the antigen-free and antigen-bound states.

Crystals of 1H7 Fab could be obtained in the presence of mannopyranoside. The structure was determined by molecular replacement at 2.8 Å resolution. Data collection and refinement statistics are provided in Table 1. Analysis of the structures of the two Fab molecules, AB and LH, in the asymmetric unit (Fig. 1 *A*) revealed that five of the six CDRs could be assigned to known classes of canonical structures (20,21): L1:2, L2:1, L3:1, H1:1, and H2:2. Although the elbow angles in the two molecules were within the reported range (127–227° (22)), they differed significantly between the two molecules; in the case of AB, it was 163°, whereas in LH, it equaled 176° (Fig. 1 *B*). Although residues of the CDRs in AB interact with both chains (L′ and H′), the paratope of LH primarily interacts with only the light chain of the symmetry-related molecule (A′; Fig. 1 *C*).

Despite large differences in the elbow angles and the nature of interacting residues of the symmetry-related molecule, the two molecules in the asymmetric unit do not differ in their CDR conformations. The orientations of most of the side chains do not show major variation, such that the surface topology of the antigen-combining sites of AB and LH are similar (Fig. 1 *C*). The superimposition of the Cα atoms of the CDR loops is depicted in Fig. 1 *D*. The RMSD for each of the six CDRs ranged from a minimum of 0.4 Å to a maximum of 0.7 Å (in the case of CDR H3). In addition, the average B-factors of the antigen binding CDR loops did not exhibit significant differences vis à vis the framework region in both AB and LH. Thus, structural similarity in the paratope of AB and LH was observed despite differences in their elbow angles and packing environments. It therefore appears that the absence of conformational and topological difference in the antigen binding site of the two molecules may be a reflection of the inherent ''rigidity'' of the antibody paratope.

TABLE 1 X-ray data collection, structure refinement, and validation statistics for 1H7 Fab crystal in the presence of the cocrystallization ligand mannopyranoside

Parameter	1H7 Fab
Space group	$P2_1$
No. of molecules in asymmetric unit	2
Cell constants (Å)	
a	40.0
b	79.7
c	132.3
β	90.7°
Resolution (Å)	50.0–2.8
Completeness (%)	95.9 (94.4)
No. of observed reflections	64,600
No. of unique reflections	19,865
Multiplicity	3.25
Average ⟨I⟩/⟨sigI⟩	7.3 (1.2)
Rmerge (%)	9.8
Matthews coefficient ($Å^3$/Dalton)	2.2
R_{free} (%)	26.7
R_{cryst} (%)	24.2
No. of solvent molecules	106
RMSD bond length	0.01
RMSD bond angle	1.76
Ramachandran plot	
Residues in allowed region	96.7%
Residues in generously allowed region	2.5%
Residues in disallowed region	0.8%

Values in parentheses correspond to the highest resolution shell.

Although the crystallization of the 1H7 Fab was in the presence of 25-fold molar excess of the mannopyranoside, the antibody crystallized, excluding the antigen. No electron density was decipherable for the carbohydrate ligand in either of the two molecules in the asymmetric unit even after adequate refinement of the crystal structure. Analysis of several carbohydrate-antibody complex structures indicated a common binding site for a monosaccharide moiety (Fig. 2 *A*; 23–29). An exhaustive search for electron density in and around the proposed common monosaccharide binding site confirmed that the 1H7 Fab was in the native unliganded state in both AB and LH. Instead, it was found that the side chain of antibody heavy-chain Tyr-106 (HTyr-106 and BTyr-106) occupied the common monosaccharide binding site (Fig. 2 *B*). Steric hindrance due to the bulky phenyl side chain probably prevented the binding of the mannopyranoside ligand during crystallization. The orientations of the side chains of HTyr-106 and BTyr-106 were apparently locked because of multiple van der Waals contacts and hydrogen bonds within the paratope and with the symmetry-related molecule (Fig. 2 *B*). Additionally, water molecules present in the vicinity also stabilize the orientation of the tyrosine side chain. Thus, crystal packing appears to secure the orientation of HTyr-106 and BTyr-106 such that 1H7 Fab crystallizes in the unliganded state despite much molar excess of mannopyranoside in the crystallization setup.

Native 1H7 Fab in the absence of any antigen also crystallized in the $P2_1$ space group with unit cell dimensions almost identical to those of the Fab cocrystallized in the presence of mannopyranoside (data not shown). The structure was determined and refined at 2.8 Å resolution and was found to be identical to the structure of 1H7 Fab crystallized in the presence of the antigen. The common orientation of HTyr-106 and BTyr-106 in the two structures reinforced the interpretations regarding the antigen-free state of the previous structure.

Structural investigations of the mimicry-recognizing mAb 2D10 by x-ray crystallography were also attempted. However, crystallization trials with either the Fab fragment or the whole immunoglobulin G molecule of mAb 2D10 were unsuccessful, probably due to the existence of multiple conformational states, in dynamic equilibrium because of the flexible nature of the antibody paratope. Alternatively,

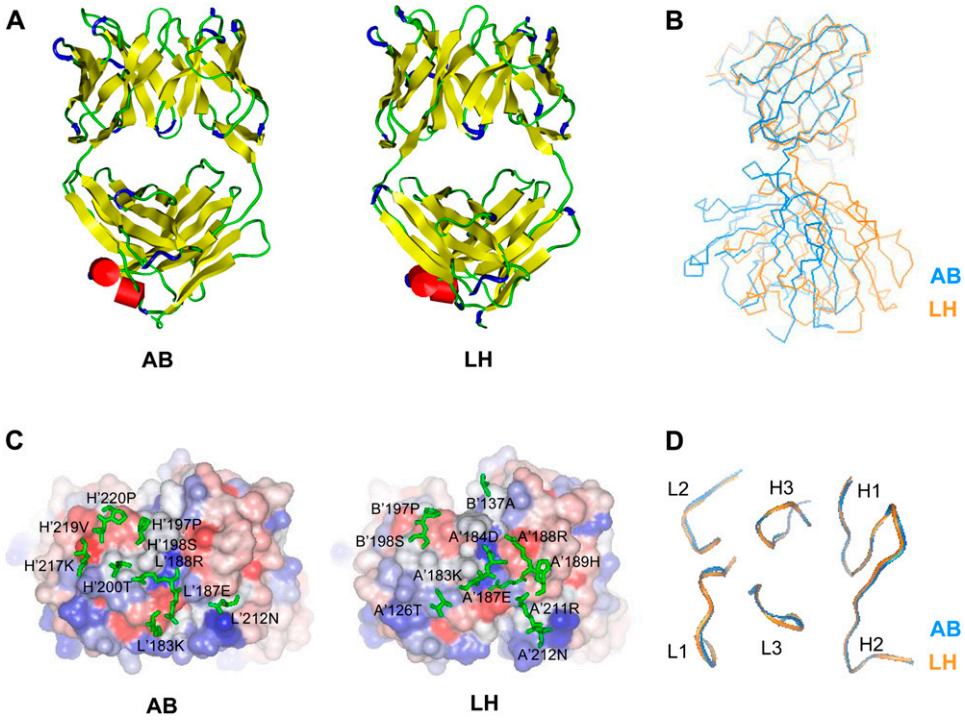

FIGURE 1 Two molecules in the asymmetric unit of 1H7 Fab crystals. (*A*) Secondary structure elements of the mAb 1H7 Fab molecules, AB and LH. β-sheets are depicted as ribbons in yellow and α-helices as cylinders in red. (*B*) Superimposition of the backbone of variable regions of the light and heavy chains of AB and LH to highlight the difference in the elbow angles of the two molecules of the asymmetric unit. (*C*) Connolly surfaces of AB and LH colored according to hydropathy emphasizing the similarity of surface topology of the two molecules of the asymmetric unit in the crystalline state. Overlaid on the surface are the residues of the symmetry-related molecules, in green, that interact (within 4 Å) with the CDR loops of AB and LH. (*D*) Ribbon representation of the six CDR loops (L1, L2, L3, H1, H2, and H3) showing the absence of structural variation between the two molecules, AB and LH. The backbone Cα atoms of the framework regions of the two molecules were superimposed to highlight the differences, if any, in the conformations of the CDR loops.

homology-based modeling of the Fv fragment of mAb 2D10 was carried out as the variable regions of the heavy and light chains of the antibody had been previously sequenced (12). Homology searches indicated that the heavy chain of mAb 2D10 shared 94.9% identity with an antibody known to cross-react between myosin and streptococcal antigens (30) and 93.2% identity with antibodies found in systemic lupus erythematosus, an autoimmune disorder (31). The light chain

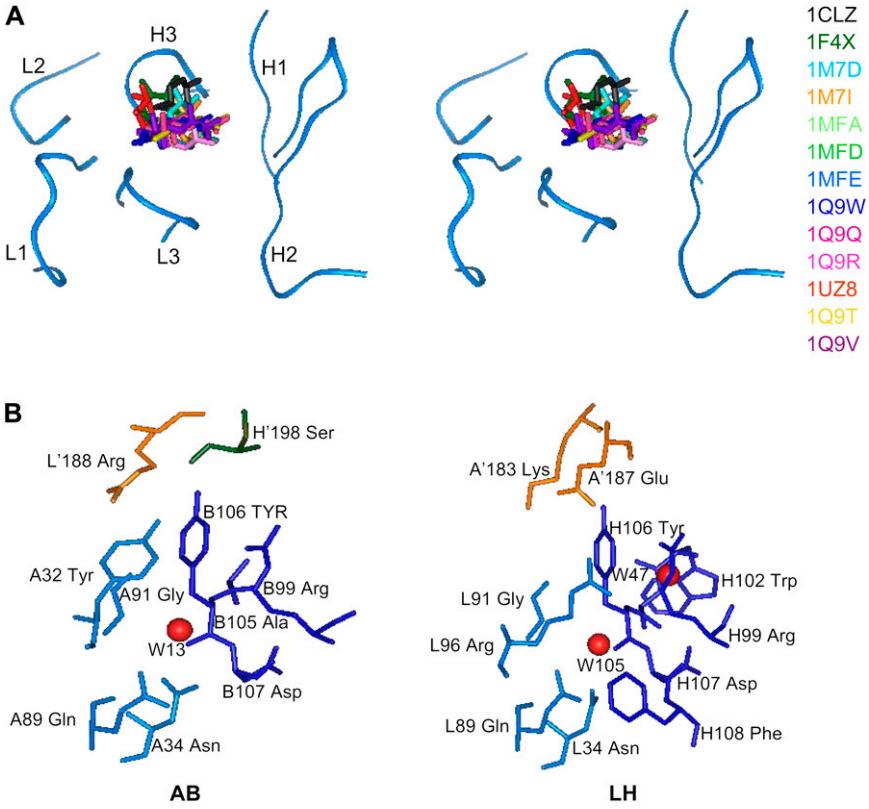

FIGURE 2 Common monosaccharide binding site in anti-carbohydrate antibodies. (*A*) Stereoscopic representation of the monosaccharide unit interacting at the common site is depicted in the context of the CDR loops of the structure of mAb 1H7. Analysis of the structures of different anti-carbohydrate antibodies in complex with oligosaccharides revealed that at least one monosaccharide unit of their respective carbohydrate ligands partially overlaps at a common site. The antibodies have been superimposed using the backbone of both light and heavy-chain framework regions. The sugars are colored according to the legend that lists the PDB accession code of their carbohydrate-antibody structures. (*B*) Environment of heavy-chain Tyr-106 of the two molecules, AB and LH, with interacting residues within 4 Å. Residues of the light and heavy chain of the same molecule are shown in light and dark blue, respectively, and those from the symmetrically related molecule are colored in orange and green, respectively. Water molecules are depicted as red spheres.

also shows high homology (99.1% identity) with autoantibodies that recognize mimicry (32). The high degree of similarity between the mimicry-recognizing mAb 2D10 and other antibodies known to be cross-reactive may have implications in the patterns of usage of V, D, and J gene segments in the context of molecular mimicry.

Model building involved the transfer of coordinates of the backbone and identical side chains of the Fv region from the anti-Digoxin (digoxigenin tridigitoxoside) antibody 26-10 (PDB ID: 1IGI) that showed 72% and 94% identity with the heavy and light chains of mAb 2D10, respectively (Fig. 3 *A*), followed by energy minimization and stereochemistry validation. Fig. 3 *B* depicts the secondary structure representation of 2D10 Fv. The six CDR loops (L1, L2, L3, H1, H2, and H3) that together form the antigen-combining site are depicted in Fig. 3 *C*. Five of the six CDRs could be assigned to the known classes of canonical structures (20,21): L1:4, L2:1, L3:1, H1:1, and H2:2. Interestingly, four of the five CDR loops of mAbs 1H7 and 2D10 belong to the same canonical class, whereas L1, which has five-residue insertion in the case of mAb 2D10, belongs to a different class.

Correlation of molecular mimicry and the conformational flexibility in the antibody paratope

Kinetic and thermodynamic analyses of binding had suggested that although the mannopyranoside-specific mAb 1H7 may have a predesigned combining site for the carbohydrate antigen, that of mAb 2D10 appeared to undergo conformational change to bind the peptide mimic as well as the carbohydrate immunogen (12). One of the approaches to image the possible conformational flexibility in the binding site of a receptor/antibody would be to carry out molecular dynamics (MD) simulation at different temperatures. Such a simulation done in the presence of solvent is a close approximation of the natural status of proteins wherein a flexible protein is likely to exist in a dynamic equilibrium of different conformational states. Toward deciphering the extent of flexibility present in the antibody paratope, MD simulations of the variable regions of mAbs 1H7 and 2D10 were carried out. The coordinates of 1H7 Fv were taken from the crystal structure of native 1H7 Fab, whereas the model of 2D10 Fv was used as the starting structure for the MD simulation.

To ascertain the degree of conformational variation extant in the two antibodies, 2 ns MD simulation was carried out at 35°C wherein greater mobility would be possible with reference to simulation at 16°C. Fig. 4 shows the comparison of the antibodies in terms of potential energy variations of the hydrated Fv molecule and the conformational fluctuations in the CDR loops across the 2 ns simulations at 16°C and 35°C. The energy profiles of the antibodies at the two temperatures do not seem to be significantly different (Fig. 4 *A*). However, the conformations of the CDR loops appear to vary considerably (Fig. 4, *B* and *C*). No significant difference is observed in the RMSD of Cα atoms of the six antigen binding loops of mAb 1H7 Fv at the two temperatures (Table 2 and Fig. 4 *B*). On the other hand, in the case of mAb 2D10, the

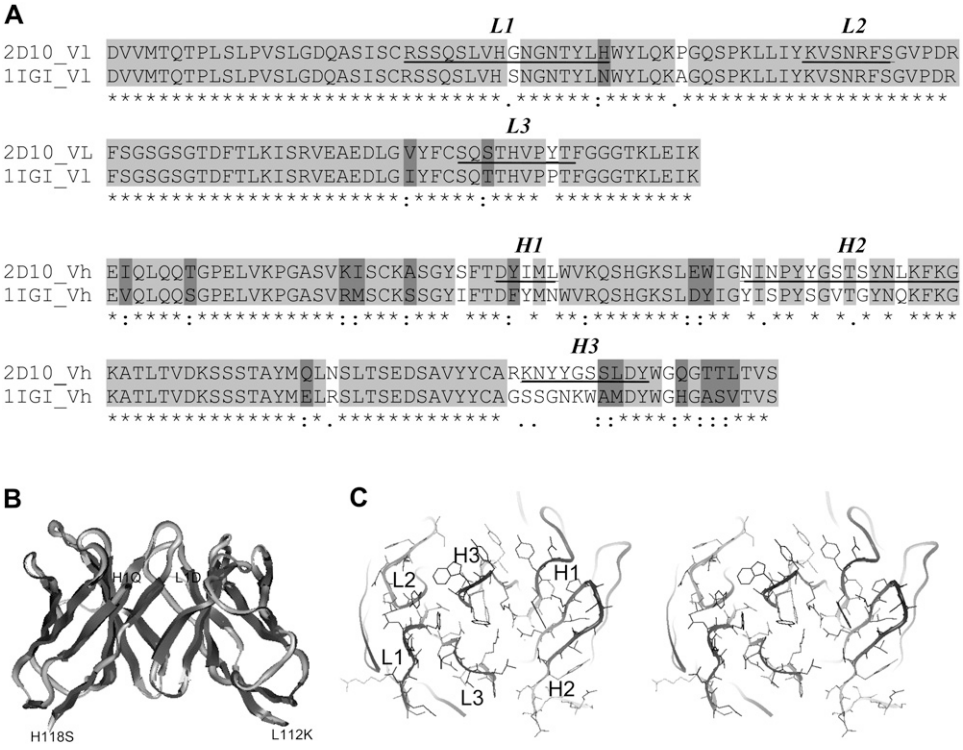

FIGURE 3 Homology modeling of 2D10 Fv. (*A*) Sequence alignment of variable region of light and heavy chains of 2D10 with 1IGI. The template for model was selected on the basis of highest homology with both chains of the antibody for optimum juxtaposition of the VL and VH domains. Although the light chain shows 94% identity, the heavy chain shares 72% identity. (*B*) Secondary structure rendition of the model of 2D10 Fv with β-sheets depicted as dark gray ribbons. (*C*) Antigen-combining site of mAb 2D10 with the six CDR loops highlighted. Orientation of the figure (*C*) is rotated by 90° with respect to the figure (*B*).

average RMSD increased appreciably: from 16°C to 35°C. Significant contribution to this variability in RMSD at 35°C in mAb 2D10 arises due to CDR L1, which has a five-residue insertion vis à vis mAb 1H7 (Fig. 4 *C*). Although the extent of variation of CDR H3, the specificity-defining loop, of 1H7 Fv either at 16°C or 35°C is comparable, greater RMSD fluctuations and conformational variability is seen in CDR H3 of mAb 2D10 in comparison with the antibody 1H7 (Table 2 and Fig. 4 *C*).

Comparative MD simulations carried out for a relatively shorter duration of 500 ps for each of the conditions provide inferences consistent with 2 ns runs despite the difference in the duration of the simulations and initial velocity (Supplementary Material Table 1 and Supplementary Material Fig. 1 *A*). Although the average RMSD fluctuations show negligible difference in the case of mAb 1H7 at either of the temperatures, for mAb 2D10 they vary significantly (Supplementary Material Fig. 1 *B*), with the difference for CDR H3, the specificity-defining loop, being exaggerated during the shorter 500 ps simulations (Supplementary Material Fig. 1 *C*).

Thus, the Fv fragments of the anti-carbohydrate antibodies were subjected to simulations at near physiological temperature (35°C) in an attempt to correlate paratope conformational flexibility with manifestation of mimicry, as suggested by thermodynamic analyses (12). Evaluation of the RMSD of Cα atoms of the CDRs was considered to be a good indicator of the degree of conformational divergence in the structures generated during the MD simulations. The extent of variation seen in the RMSD of the Cα atoms of the CDRs of mAb 2D10 vis à vis mAb 1H7 at 35°C reinforces that the antigen binding site of mAb 2D10 possesses flexibility whereas that of mAb 1H7 is rigid. This flexibility within the mAb 2D10 paratope compared to mAb 1H7 seems to be

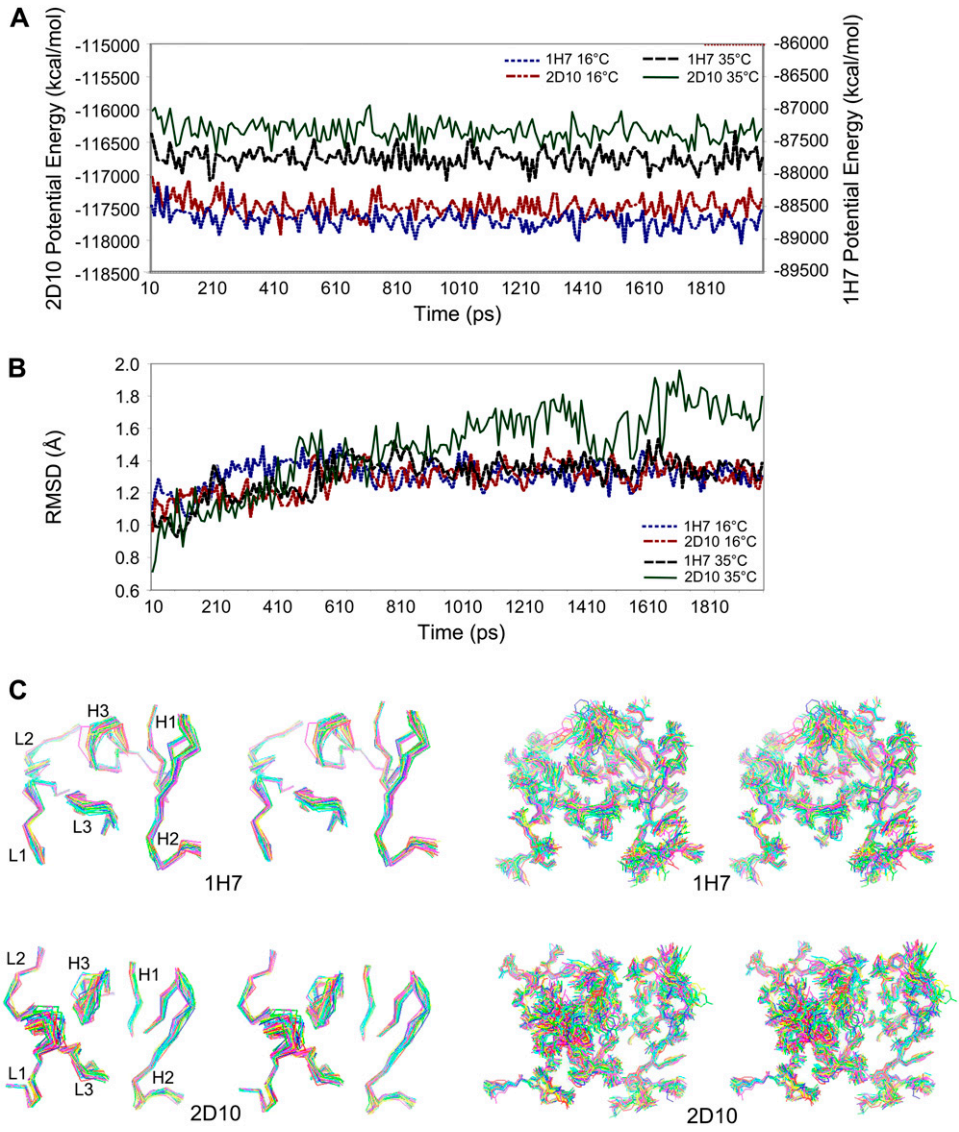

FIGURE 4 MD simulation to investigate the extent of conformational flexibility in the antigen-combining sites of the anti-mannopyranoside antibodies. (*A*) Potential energy profile of 1H7 and 2D10 Fv during simulation. The framework regions of the different structures were superimposed to highlight the extent of variation in the CDR conformations across the simulation. (*B*) RMSD of backbone Cα atoms of the CDR loops during MD simulation of 1H7 and 2D10 Fv at 16°C and 35°C, with all six CDRs together. Maximum variation in the CDR backbone conformation is seen in the case of 2D10 Fv at 35°C. (*C*) Stereoscopic representation of the Cα trace (*left*) and heavy atoms (*right*) of the CDRs of the structures output every 50 ps from the MD simulation of 1H7 Fv (*top*) and 2D10 Fv (*bottom*) at 35°C, superimposed with respect to the framework region.

TABLE 2 Average fluctuation in RMSD of Cα atoms of the CDR loops of the anti-mannopyranoside antibodies during MD simulations for a duration of 2 ns

	Average RMSD Fluctuations (Å)			
	All CDRs		CDR H3	
	mAb 1H7	mAb 2D10	mAb 1H7	mAb 2D10
16°C	1.21 (±0.07)	1.17 (±0.12)	1.59 (±0.19)	1.48 (±0.25)
35°C	1.16 (±0.11)	1.41 (±0.38)	1.84 (±0.36)	2.09 (±0.57)

Structures output every 10 ps were superimposed with respect to the framework region. Values in parentheses represent the standard deviation.

correlated with the intramolecular contacts within the CDRs; there exist 27 hydrogen bonds within the antigen-combining site of mAb 1H7 vis à vis 8 within mAb 2D10.

Conformational states of the antibody paratope and antigen binding modes

Structural analyses of the molecular complexes of the two antibodies, 1H7 and 2D10, with the carbohydrate immunogen would enable the understanding of the role of conformational flexibility in their antigen recognition potential. Such an analysis was accomplished by in silico docking of the mannopyranoside antigen in the paratope of the two antibodies.

In the crystal structure of 1H7 Fab, the tyrosine side chain of H106 was found to be occupying the common monosaccharide binding site—which may be defined as the primary site—in anti-carbohydrate antibodies (Fig. 2 *A*). Thus, it can be envisioned that for mannopyranoside to be docked in the 1H7 antibody paratope guided by the position of the common binding site, an alternate conformation for the heavy-chain Tyr-106 side chain needed to be searched. Energy needed for such a change in the orientation of the side chain is likely to be negligible and was reflected in the thermodynamic analyses (12). Furthermore, to validate the alternate heavy-chain Tyr-106 rotamer, MD simulation of the structure was carried out, at 35°C, and the HTyr-106 side chain was found to be stable in the alternate orientation during the 500 ps simulation.

To determine the possible modes of binding of the carbohydrate immunogen, docking by AUTODOCK3.05 (19) of the mannopyranoside antigen on 1H7 Fv with the altered conformation for heavy-chain Tyr-106 was attempted. Multiple structures output from the MD simulation every 50 ps were used for the docking analysis. Fig. 5 *A* depicts the superimposition of the individual docking options output with the different structures of 1H7 Fv. There appears to be a single mannopyranoside docking site that dominates the antibody paratope which also overlaps with the proposed common monosaccharide binding site. Although, the relative orientations of the carbohydrate ligand at this dominant site differ, the docking energies of the various options are within a narrow range. Interestingly, the AUTODOCK3.05 analysis involving mannopyranoside and the 1H7 with the crystallographically obtained orientation of the heavy-chain Tyr-106 did not show similar binding of the carbohydrate antigen.

AUTODOCK3.05 was also used for docking mannopyranoside in the paratope of antibody 2D10 toward analyzing the possible sites and modes of interaction with the carbohydrate immunogen. It was hypothesized that the flexibility in the binding site may be utilized for the recognition of diverse ligands with similar affinity. Docking parameters, including grid size selected for the conformational space exploration, were identical to those used in the case of mAb 1H7. The docking options from the individual runs of AUTODOCK3.05 are depicted in Fig. 5 *A* along with their respective antibody paratopes. Consistent with expectations, the mannopyranoside ligand is docked at multiple locations within the antigen binding site. However, one of the dominant sites overlaps with the common monosaccharide binding

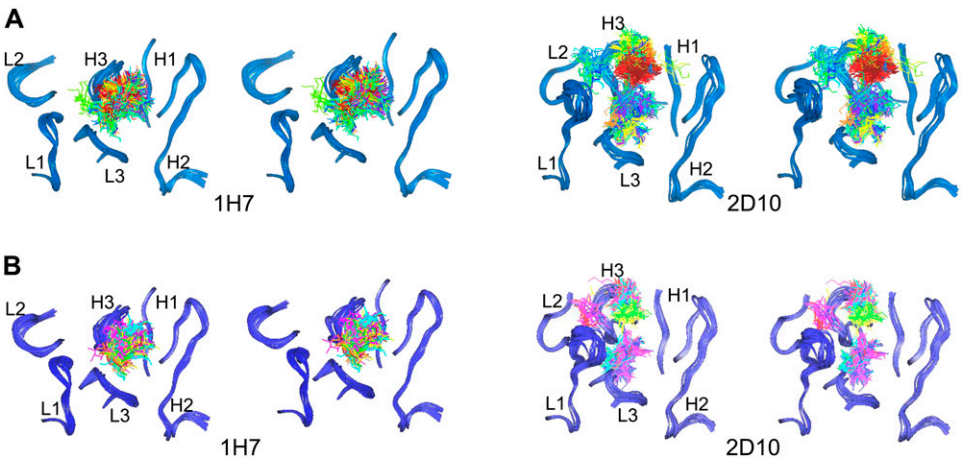

FIGURE 5 Stereoscopic representation of the docking of monosaccharides within the paratope of the antibodies, 1H7 and 2D10. Antigen-combining site of mAb 1H7 (*left*) and mAb 2D10 (*right*) with the various docking options of (*A*) mannopyranoside and (*B*) glucopyranoside generated during the individual runs of AUTODOCK3.05. Structures that were output every 50 ps during the 500 ps MD simulation at 35°C were selected for the automated docking of each monosaccharide. Each run of AUTODOCK3.05 generated 100 different docking options, and only those that juxtaposed within the antibody paratope were selected. All docking options from a run of AUTODOCK3.05 are colored similarly and shown in the context of the CDR loops of their respective antibody structures. The different structures of each antibody generated during the simulation are superimposed with respect to the framework regions to depict variation, if any, in the CDR loops.

site. The presence of additional binding sites may explain the ability of the antibody to recognize diverse sugars. To test this, we analyzed the binding of methyl-α-D-glucopyranoside, which had been shown to bind to mAb 2D10 with equivalent affinity and with significantly lower affinity to mAb 1H7 (12). Consistent with experimental data, the average docking energy for both mannopyranoside and glucopyranoside are similar in the case of 2D10, whereas for mAb 1H7 it is considerably higher for glucopyranoside than for mannopyranoside (Table 3). Additionally, whereas glucopyranoside binds at a single site, overlapping with the proposed common monosaccharide binding site within the 1H7 paratope, it can dock at multiple sites that overlap with the mannopyranoside binding sites within the 2D10 paratope (Fig. 5 *B*).

DISCUSSION

The vast recognition repertoire of the immune system while maintaining exquisite specificity of the response against any invading antigen is, indeed, remarkable. Breakdown in this specificity, however, manifests as molecular mimicry. We attempted to delineate the mechanisms of binding of independent yet mimicking antigens to anti-carbohydrate antibodies that differed in their recognition potential; whereas mAb 1H7 was specific to the immunizing mannopyranoside alone, mAb 2D10 could recognize 12-mer peptide in addition to the carbohydrate moiety. The kinetic and thermodynamic studies have indicated the role of paratope conformational flexibility in the binding of antigens that mimic one another (12). In addition to deciphering the structural features of the paratope critical for mimotope recognition, our studies demonstrate diversity in antigen binding modes and interactions.

The crystal structure of 1H7 Fab revealed no significant dissimilarity in antigen-combining sites of the two molecules in the asymmetric unit, indicating structural invariance in the antibody paratope. Despite differences in the packing environments of the two molecules, the RMSD of the Cα atoms of the six CDR loops was not substantial, and most side chains were in a similar orientation. Interestingly, the aromatic side chain of the antibody heavy-chain Tyr-106 overlaps with the common monosaccharide binding site. We defined this common site based on comparative analysis of the structures of various anti-carbohydrate antibodies in complex with their respective saccharide antigens. It was therefore reasonable to expect that such an orientation of the heavy-chain Tyr-106 residue, stabilized by interactions both within the paratope and due to crystal packing, sterically obstructs the binding of mannopyranoside. This probably resulted in the crystallization of 1H7 Fab in the unliganded state even though cocrystallization was set up with 25 molar excess of mannopyranoside. Comparison of the structural features of the antigen-combining sites of mAbs 2D10 and 1H7 showed that the CDR loops of the two antibodies belong to the same class of canonical structures, with the exception of L1 which has a five-residue insertion in the case of mAb 2D10.

TABLE 3 Average estimated docking energy for monosaccharides binding to anti-mannopyranoside antibodies

	Average docking energy (kcal/mol)	
	1H7	2D10
Mannopyranoside	−6.9 (±0.3)	−7.1 (±0.6)
Glucopyranoside	−5.7 (±0.3)	−6.8 (±0.3)

Of the 100 different options of either monosaccharide docked onto different structures of mAbs 1H7 and 2D10 output every 50 ps during the 500 ps MD simulation, the lowest docking energies were averaged. Values in parentheses represent the standard deviation.

The importance of topological equivalence between chemically unrelated moieties for functional mimicry has been suggested (33–35). However, we have demonstrated that functional mimicry can be observed in the context of antibody response even in the absence of obvious structural correlation between the independent ligands (10,11). Indications of a possible alternate mode of recognition of mimicking antigens by utilizing conformational flexibility of the ligand binding site arose from our kinetic and thermodynamic analyses (12). MD simulation provides an elegant window to observe the structural dynamics of a range of possible conformations inherent in the protein molecule. MD simulations at different temperatures revealed significantly greater variation in the RMSD of the Cα atoms of the CDR loops, importantly in CDR H3, in the case of mimicry-recognizing antibody 2D10 vis à vis the immunogen-specific mAb 1H7. Indeed, the structural investigations reported in this study substantiate the premise that mAb 2D10 exhibits conformational flexibility in the antigen-combining site. On the other hand, the antibody 1H7 shows relatively low structural mobility in the paratope.

The structural basis of the conformational fluctuations in the loops of 2D10 as against 1H7 was analyzed. While addressing the cause for the differential binding potential of the two antibodies, we had previously analyzed the differences in the nature of the residues lining the antigen-combining site of the antibodies (12). We could not, however, attribute any significant difference in the nature of residues of the paratope to differences in their recognition repertoire despite CDR L1 of 2D10 having a five-residue insertion as compared to 1H7. This analysis based on MD simulations demonstrated that the conformational variability within the antigen binding site of 2D10 is contributed by both CDR L1, which has a five-residue insertion in the case of 2D10, and CDR H3, which has a physiologically critical role in defining specificity. Interestingly, there are three times as many intramolecular hydrogen bonds within the antigen-combining site of mAb 1H7 as compared to mAb 2D10.

The correlation of the structural features of the antibody paratope with differential modes of antigen binding was established by analyzing the nature of the interactions involved. It was pertinent to discern whether the conformational flexibility demonstrated by the simulation studies might be

reflected in the recognition repertoire of these antibodies. Automated docking of mannopyranoside, based on the energy of the interactions between the ligand and the receptor, should reveal all the potential carbohydrate binding sites within the antibody paratope. Consistent with expectations, upon altering the side-chain orientation of HTyr-106 (BTyr-106), which was hindering ligand access, mannopyranoside could snugly dock in the antibody 1H7 paratope. This docking site overlaps with the proposed common primary monosaccharide binding site present in other anti-sugar antibodies in complex with oligosaccharides.

The automated docking onto mAb 2D10 revealed that mannopyranoside could bind at additional sites besides the common primary monosaccharide binding site. The existence of multiple binding modes within the antibody paratope appears to be a direct outcome of the conformational adoptability of the antibody. The presence of multiple conformational states in dynamic equilibrium may expose buried surfaces that act as potential/additional binding sites for the carbohydrate antigen. The binding of other sugars like glucopyranoside at the common monosaccharide binding site, albeit with lower affinity, in the case of mAb 1H7 and multiple equivalent binding modes for mAb 2D10 supports our inferences regarding the ability of the mimicry-recognizing antibody to bind two independent antigens utilizing the intrinsic flexibility in the antigen-combining site.

It has been proposed that affinity maturation involves the evolution of the antibody paratope to reduce its inherent flexibility and toward epitope complementarity, resulting in a well-defined binding site for the immunogen in mature antibodies (36,37). However, our studies demonstrate that an immune response generated in the context of molecular mimicry includes not only antibodies like 1H7, which have narrow specificity, but also those like mAb 2D10, which possess paratope conformational flexibility and facilitate recognition of mimotopes despite an imperfect topological relationship. Physiologically, this may be important; when pathogens evade immune surveillance by changing their antigenic determinants, the immune system needs to recognize altered antigens despite their structural differences. Responses under such conditions therefore may include antibody receptors with broader recognition specificities. A certain proportion of secondary antibodies that possess conformational flexibility, exemplified by mAb 2D10, are probably designed to disregard antigenic variation. At the same time, antibodies like mAb 1H7 that have acquired the ability to discriminate ensure high specificity of the mature immune response. Thus, our studies reflect the diversity in the immune response at the structural level, even against small immunogens such as mannopyranoside. The antibodies not only show sequence variation due to independent germ line origins and differences in their thermodynamic characteristics of antigen binding, but also exhibit diversity in terms of the structural properties of the paratope which is reflected as multiple antigen recognition modes.

In summary, we suggest that alternate mechanisms of enhancement of the recognition repertoire exist in the mature immune response that manifest as molecular mimicry even in the absence of well-defined structural similarity. Our investigations of the mechanisms by which the immune system addresses molecular equivalences suggest that fidelity of recognition of the response is maintained by antibodies that have a rigid and predesigned binding site for the immunizing antigen, and the antibodies which possess paratope conformational flexibility ensure a sufficiently large repertoire of specificities. Thus, the receptor-specific modulations of molecular mimicry perhaps reflect strategies evolved by the adaptive immune system to counter the changing surface properties of invading pathogens.

SUPPLEMENTARY MATERIAL

To view all of the supplemental files associated with this article, visit www.biophysj.org.

We thank Drs. D. Mohanty and D. K. Sethi for useful discussions.

This work was supported by the Department of Biotechnology, government of India. L.K. is a recipient of a fellowship from the Council of Scientific and Industrial Research (India).

REFERENCES

1. Baum, H., P. Butler, H. Davies, M. J. Sternberg, and A. K. Burroughs. 1993. Autoimmune disease and molecular mimicry: a hypothesis. *Trends Biochem. Sci.* 18:140–144.
2. Ray, S. K., C. Putterman, and B. Diamond. 1996. Pathogenic autoantibodies are routinely generated during the response to foreign antigen: a paradigm for autoimmune disease. *Proc. Natl. Acad. Sci. USA.* 93:2019–2024.
3. Stebbins, C. E., and J. E. Galan. 2001. Structural mimicry in bacterial virulence. *Nature.* 412:701–705.
4. Agadjanyan, M., P. Luo, M. A. Westerink, L. A. Carey, W. Hutchins, Z. Steplewski, D. B. Weiner, and T. Kieber-Emmons. 1997. Peptide mimicry of carbohydrate epitopes on human immunodeficiency virus. *Nat. Biotechnol.* 15:547–551.
5. Harris, S. L., L. Craig, J. S. Mehroke, M. Rashed, M. B. Zwick, K. Kenar, E. J. Toone, N. Greenspan, F. I. Auzanneau, J. R. Marino-Albernas, B. M. Pinto, and J. K. Scott. 1997. Exploring the basis of peptide-carbohydrate crossreactivity: evidence for discrimination by peptides between closely related anti-carbohydrate antibodies. *Proc. Natl. Acad. Sci. USA.* 94:2454–2459.
6. Jain, D., K. J. Kaur, B. Sundaravadivel, and D. M. Salunke. 2000. Crystal structure of a carbohydrate-mimicking peptide bound to concanavalin A. *J. Biol. Chem.* 275:16098–16102.
7. Jain, D., K. J. Kaur, M. Goel, and D. M. Salunke. 2000. Structural basis of functional mimicry between carbohydrate and peptide ligands of Con A. *Biochem. Biophys. Res. Commun.* 272:843–849.
8. Jain, D., K. J. Kaur, and D. M. Salunke. 2001. Plasticity in protein-peptide recognition: crystal structures of two different peptides bound to concanavalin A. *Biophys. J.* 80:2912–2921.
9. Jain, D., K. J. Kaur, and D. M. Salunke. 2001. Enhanced binding of a rationally designed peptide ligand of concanavalin A arises from improved geometrical complementarity. *Biochemistry.* 40:12059–12066.
10. Kaur, K. J., S. Khurana, and D. M. Salunke. 1997. Topological analysis of the functional mimicry between a peptide and a carbohydrate moiety. *J. Biol. Chem.* 272:5539–5543.

11. Kaur, K. J., D. Jain, M. Goel, and D. M. Salunke. 2001. Immunological implications of structural mimicry between a dodecapeptide and a carbohydrate moiety. *Vaccine*. 19:3124–3130.

12. Goel, M., L. Krishnan, S. Kaur, K. J. Kaur, and D. M. Salunke. 2004. Plasticity within the antigen-combining site may manifest as molecular mimicry in the humoral immune response. *J. Immunol.* 173:7358–7367.

13. Navaza, J. 1994. AMoRe: an automated package for molecular replacement. *Acta Crystallogr. A.* 50:157–163.

14. Brunger, A. T., P. D. Adams, G. M. Clore, W. L. DeLano, P. Gros, and R. W. Grosse-Kunstleve. 1998. Crystallography and NMR system: a new software suite for macromolecular structure determination. *Acta Crystallogr. D Biol. Crystallogr.* 54:905–921.

15. Brunger, A. T. 1993. Assessment of phase accuracy by cross validation: the free R value. Methods and applications. *Acta Crystallogr. D Biol. Crystallogr.* 49:24–36.

16. Jones, T. A., J. Y. Zou, S. W. Cowan, and M. Kjeldgaard. 1991. Improved methods for building protein models in electron-density maps and the location of errors in these models. *Acta Crystallogr. A.* 47:110–119.

17. Laskowski, R. A., M. W. MacArthur, D. S. Moss, and J. M. Thornton. 1993. PROCHECK: a program to check the stereochemical quality of protein structures. *J. Appl. Cryst.* 26:283–291.

18. Case, D. A., D. A. Pearlman, J. W. Caldwell, T. E. Cheatham 3rd, J. Wang, W. S. Ross, C. L. Simmerling, T. A. Darden, K. M. Merz, R. V. Stanton, A. L. Cheng, J. J. Vincent, M. Crowley, V. Tsui, H. Gohlke, R. J. Radmer, Y. Duan, J. Pitera, I. Massova, G. L. Seibel, U. C. Singh, P. K. Weiner, and P. A. Kollman. 2002. AMBER 7, University of California, San Francisco.

19. Morris, G. M., D. S. Goodsell, R. S. Halliday, R. Huey, W. E. Hart, R. K. Belew, and A. J. Olson. 1998. Automated docking using a lamarckian genetic algorithm and empirical binding free energy function. *J. Comput. Chem.* 19:1639–1662.

20. Chothia, C., and A. M. Lesk. 1987. Canonical structures for the hypervariable loops of immunoglobulins. *J. Mol. Biol.* 196:901–917.

21. Chothia, C., A. M. Lesk, A. Tramontano, M. Levitt, S. J. Smith-Gill, G. Air, S. Sheriff, E. A. Padlan, D. Davies, W. R. Tulip, P. M. Colman, S. Spinelli, P. M. Alzari, and R. J. Poljak. 1989. Conformations of immunoglobulin hypervariable regions. *Nature*. 342:877–883.

22. Padlan, E. A. 1996. X-ray crystallography of antibodies. *Adv. Protein Chem.* 49:57–133.

23. Villeneuve, S., H. Souchon, M. M. Riottot, J. C. Mazie, P. S. Lei, C. P. J. Glaudemans, P. Kovac, J. M. Fournier, and P. M. Alzari. 2000. Crystal structure of an anti-carbohydrate antibody directed against *Vibrio cholera* O1 in complex with antigen: molecular basis for serotype specificity. *Proc. Natl. Acad. Sci. USA.* 97:8433–8438.

24. Nguyen, H. P., N. O. Seto, C. R. MacKenzie, L. Brade, P. Kosma, H. Brade, and S. V. Evans. 2003. Germline antibody recognition of distinct carbohydrate epitopes. *Nat. Struct. Biol.* 10:1019–1025.

25. Zdanov, A., Y. Li, D. R. Bundle, S. J. Deng, C. R. MacKenzie, S. A. Narang, N. M. Young, and M. Cygler. 1994. Structure of a single-chain antibody variable domain (Fv) fragment complexed with a carbohydrate antigen at 1.7 Å resolution. *Proc. Natl. Acad. Sci. USA.* 91:6423–6427.

26. Vyas, N. K., M. N. Vyas, M. C. Chervenak, M. A. Johnson, B. M. Pinto, D. R. Bundle, and F. A. Quiocho. 2002. Molecular recognition of oligosaccharide epitopes by a monoclonal Fab specific for shigella flexneri Y lippopolysaccharide: x-ray structures and thermodynamics. *Biochemistry.* 41:13575–13586.

27. Jeffrey, P. D., J. Bajorath, C. Y. Chang, D. Yelton, I. Hellstrom, K. E. Hellstrom, and S. Sheriff. 1995. The x-ray structure of an anti-tumour antibody in complex with antigen. *Nat. Struct. Biol.* 2:466–471.

28. Bundle, D. R., H. Baumann, J. R. Brisson, S. M. Gagne, A. Zdanov, and M. Cygler. 1994. Solution structure of a trisaccharide-antibody complex: comparison of NMR measurements with a crystal structure. *Biochemistry.* 33:5183–5192.

29. Cygler, M., D. R. Rose, and D. R. Bundle. 1991. Recognition of a cell-surface oligosaccharide of pathogenic Salmonella by an antibody Fab fragment. *Science*. 253:442–445.

30. Mertens, N. M., J. E. Galvin, E. E. Adderson, and M. W. Cunningham. 2000. Molecular analysis of cross-reactive anti-myosin/anti-streptococcal mouse monoclonal antibodies. *Mol. Immunol.* 37:901–913.

31. Kofler, R., R. Strohal, R. S. Balderas, M. E. Johnson, D. J. Noonan, M. A. Duchosal, F. J. Dixon, and A. N. Theofilopoulos. 1988. Immunoglobulin kappa light chain variable region gene complex organization and immunoglobulin genes encoding anti-DNA autoantibodies in lupus mice. *J. Clin. Invest.* 82:852–860.

32. Putterman, C., B. Deocharan, and B. Diamond. 2000. Molecular analysis of the autoantibody response in peptide-induced autoimmunity. *J. Immunol.* 164:2542–2549.

33. Goel, M., D. Jain, K. J. Kaur, R. Kenoth, B. G. Maiya, M. J. Swamy, and D. M. Salunke. 2001. Functional equality in the absence of structural similarity: an added dimension to molecular mimicry. *J. Biol. Chem.* 276:39277–39281.

34. Nair, D. T., K. J. Kaur, K. Singh, P. Mukherjee, D. Rajagopal, A. George, V. Bal, S. Rath, K. V. Rao, and D. M. Salunke. 2003. Mimicry of native peptide antigens by the corresponding retro-inverso analogs is dependent on their intrinsic structure and interaction propensities. *J. Immunol.* 170:1362–1373.

35. Kohm, A. P., K. G. Fuller, and S. D. Miller. 2003. Mimicking the way to autoimmunity: an evolving theory of sequence and structural homology. *Trends Microbiol.* 11:101–105.

36. Wedemayer, G. J., P. A. Patten, L. H. Wang, P. G. Schultz, and R. C. Steven. 1997. Structural insights into the evolution of an antibody combining site. *Science*. 276:1665–1669.

37. Manivel, V., N. C. Sahoo, D. M. Salunke, and K. V. Rao. 2000. Maturation of an antibody response is governed by modulations in flexibility of the antigen-combining site. *Immunity*. 13:611–620.